Journal of Biotechnology 205 (2015) 36–46

Contents lists available at ScienceDirect

Journal of Biotechnology

journal homepage: www.elsevier.com/locate/jbiotec

A multi-organ chip co-culture of neurospheres and liver equivalents for long-term substance testing

Eva-Maria Materne[a,*,1], Anja Patricia Ramme[a,1], Ana Paula Terrasso[b,c], Margarida Serra[b,c], Paula Marques Alves[b,c], Catarina Brito[b,c], Dmitry A. Sakharov[d], Alexander G. Tonevitsky[e], Roland Lauster[a], Uwe Marx[a,f]

[a] Technische Universität Berlin, Institute of Biotechnology, Gustav-Meyer-Allee 25, Berlin 13355, Germany
[b] iBET, Instituto de Biologia Experimental e Tecnológica, Oeiras 2780-901, Portugal
[c] ITQB-UNL, Instituto de Tecnologia Química e Biológica, Universidade Nova de Lisboa, 2780-157 Oeiras, Portugal
[d] Scientific Research Centre Bioclinicum, Ugreshskaya ul. 2/85, 115088 Moscow, Russia
[e] Institute of General Pathology and Pathophysiology, Russian Academy of Medical Science, Baltiyskaya ul. 8, 125315 Moscow, Russia
[f] TissUse GmbH, Markgrafenstr. 18, 15528 Spreenhagen, Germany

ARTICLE INFO

Article history:
Received 9 September 2014
Received in revised form 23 January 2015
Accepted 2 February 2015
Available online 9 February 2015

Keywords:
Multi-organ-chip
Organoids
Tissue engineering
In vitro substance testing
Liver
Neurospheres

ABSTRACT

Current *in vitro* and animal tests for drug development are failing to emulate the systemic organ complexity of the human body and, therefore, often do not accurately predict drug toxicity, leading to high attrition rates in clinical studies (Paul et al., 2010). The phylogenetic distance between humans and laboratory animals is enormous, this affects the transferability of animal data on the efficacy of neuroprotective drugs. Therefore, many neuroprotective treatments that have shown promise in animals have not been successful when transferred to humans (Dragunow, 2008; Gibbons and Dragunow, 2010). We present a multi-organ chip capable of maintaining 3D tissues derived from various cell sources in a combined media circuit which bridges the gap in systemic and human tests. A steady state co-culture of human artificial liver microtissues and human neurospheres exposed to fluid flow over two weeks in the multi-organ chip has successfully proven its long-term performance. Daily lactate dehydrogenase activity measurements of the medium and immunofluorescence end-point staining proved the viability of the tissues and the maintenance of differentiated cellular phenotypes. Moreover, the lactate production and glucose consumption values of the tissues cultured indicated that a stable steady-state was achieved after 6 days of co-cultivation. The neurospheres remained differentiated neurons over the two-week cultivation in the multi-organ chip, proven by qPCR and immunofluorescence of the neuronal markers βIII-tubulin and microtubule-associated protein-2. Additionally, a two-week toxicity assay with a repeated substance exposure to the neurotoxic 2,5-hexanedione in two different concentrations induced high apoptosis within the neurospheres and liver microtissues, as shown by a strong increase of lactate dehydrogenase activity in the medium. The principal finding of the exposure of the co-culture to 2,5-hexanedione was that not only toxicity profiles of two different doses could be discriminated, but also that the co-cultures were more sensitive to the substance compared to respective single-tissue cultures in the multi-organ-chip. Thus, we provide here a new *in vitro* tool which might be utilized to predict the safety and efficacy of substances in clinical studies more accurately in the future.

1. Introduction

The development of new drugs is strikingly expensive, time-consuming and only a few substances can stand up to the long testing phase. Animal tests often fail to forecast the effects of new drugs, because the phylogenetic distance between laboratory animals and humans is too great (Bailey et al., 2013; Dragunow, 2008). The large quantities of laboratory animals used for substance testing are not only expensive and laborious, but are also ethically questionable. Therefore, it is essential to find new technologies to

* Corresponding author at: Technische Universität Berlin, Medical Biotechnology, TIB 4/4-2, Gustav-Meyer-Allee 25, 13355 Berlin, Germany. Tel.: +49 30 31427907.
E-mail addresses: eva-maria.materne@tu-berlin.de (E.-M. Materne), anja.ramme@tu-berlin.de (A.P. Ramme), aterrasso@itqb.unl.pt (A.P. Terrasso), mserra@ibet.pt (M. Serra), marques@ibet.pt (P.M. Alves), anabrito@itqb.unl.pt (C. Brito), dimitri_sakharov@mail.ru (D.A. Sakharov), tonevitsky@mail.ru (A.G. Tonevitsky), roland.lauster@tu-berlin.de (R. Lauster), uwe.marx@tu-berlin.de (U. Marx).
[1] These authors contributed equally.

http://dx.doi.org/10.1016/j.jbiotec.2015.02.002
0168-1656/

evaluate potential drug candidates at an early stage of the process. Microfluidic culture devices combining human microtissues in an organ-like arrangement at a homeostatic steady-state could well become a translational solution for that testing dilemma.

Currently, there are very few microfluidic platforms available which mimic the human situation *in vivo* (Hwan et al., 2009; Zhang et al., 2009). The disadvantages of most of these systems are the external pump and external media container, leading to a high fluid-to-tissue ratio. Thus, the crosstalk between tissues is not ensured. Furthermore, the exposure time of substances or drugs to most of these microfluidic systems ranges between 24 and 72 h, and only a few can operate up for to seven days (Marx et al., 2012). However, the Organization for Economic Co-operation and Development guidelines for toxicity testing of chemicals and cosmetics in animals require a 28-day repeated dose exposure.

Here we evaluated whether the microfluidic multi-organ chip (MOC) platform developed in our laboratory is able to co-cultivate neurospheres and liver spheroids over prolonged culture periods. The MOC, covering the area of an object slide, contains an on-chip micropump and is capable of interconnecting two different organ equivalents. The micropump ensures a stable long-term circulation of media through the tissue culture compartments at variable flow rates, adjustable to mimic blood flow-dependent mechanical shear stress in the respective tissues (Schimek et al., 2013). The tissue culture compartments and the connecting channels are optically accessible, thus, supporting live tissue imaging. We show here that the MOC is able to support co-cultures of human liver spheroids, consisting of differentiated HepaRG cells and human hepatic stellate cells, and differentiated neurospheres, derived from the NT2 cell line, over weeks at a steady-state in a combined media circuit. The differentiated phenotype of the cells was preserved, as shown by immunofluorescence staining and qRT-PCR of selected marker genes. Furthermore, the system layout and chip design support repeated substance exposure for safety or efficacy test assay development.

In a two-week toxicity assay 2,5-hexanedione was used to study it's toxic effect on the tissues. In the human liver n-hexane is either metabolized to 1-hexanol or 3-hexanol in a detoxification pathway, or in a bio-activation pathway to 2-hexanol. The 2-hexanol is further metabolized in many oxidation steps into 2,5-hexanedione and other metabolites (Yin et al., 2013). Those are distributed into the bloodstream and reach other organs as kidney and brain. 2,5-hexanedione is the main component leading to neurotoxicity, because it has the longest retention period in the human body in comparison to the other metabolites. 2,5-hexanedione can structurally change neurofilaments by pyrrole adduct formation and resulting covalent cross-linking (Heijink et al., 2000). The neurotoxic effect has been shown in different studies on laboratory animals and cell lines (DeCaprio et al., 1988; Ladefoged et al., 1994). However, a four hour exposure of 2,5-hexanedione on neuronal (NT-2-N, SK-N-H) and non-neuronal cells (NT-2) did not show any cytotoxicity, but a 24 h exposure of 32 mM 2,5-hexanedione led to toxic effects on both cell types (Woehrling et al., 2006).

2. Materials and methods

2.1. Cell sources and maintenance

Cell culture components were purchased from PAA Laboratories (GE Healthcare Europe GmbH, Vienna, Austria) and cultures were incubated in HepaRG medium at 37 °C and 5% CO_2, unless otherwise stated. HepaRG cells were obtained from Biopredic International (Rennes, France) and maintained as described by Gripon et al. (2002). Briefly, cells were cultured in HepaRG medium, consisting of William's Medium E supplemented with 10% (v/v) fetal bovine serum (FBS), 100 units ml^{-1} penicillin, 100 $\mu g\,ml^{-1}$ streptomycin, 5 $\mu g\,ml^{-1}$ human insulin, 2 mM L-glutamine, and 5×10^{-5} M hydrocortisone hemisuccinate (Sigma-Aldrich, St. Louis, MO, USA). Undifferentiated cells were maintained in 75 cm^2 tissue culture flasks (Greiner Bio One, Germany) at a seeding density of 2×10^4 cells cm^{-2} for two weeks. Induction of differentiation was initiated by allowing the cells to reach confluence by maintaining the cells in growth medium for two weeks. Differentiation medium containing 2% (v/v) dimethyl sulfoxide (DMSO; Carl Roth GmbH, Karlsruhe, Germany) was then added for another two weeks. Human hepatic stellate cells (HHSteC) and their culture supplements were purchased from ScienCell Research Laboratories (Carlsbad, CA, USA). The cells were seeded at 5×10^3 cells cm^{-2} in poly-L-lysine-coated 75 cm^2 tissue culture flasks in stellate cell medium for maintenance, according to the manufacturer's instructions. Medium was exchanged every two to three days. Cells were harvested for further use at 90% confluence. NTera-2/cl.D1 (NT2) cells were obtained from American Type Cell Culture Collection (ATCC) and maintained as described by Brito et al. (2007). Briefly, undifferentiated cells were routinely cultured at a seeding density of 4–4.5 $\times 10^4$ cell cm^{-2} in DMEM, supplemented with 10% (v/v) FBS and 1% (v/v) penicillin-streptomycin (P/S; all purchased from Invitrogen).

2.2. Preparation of neurospheres and liver microtissues

Preparation of neurospheres was performed as described in Serra et al. (2009). Briefly, a single cell suspension of undifferentiated NT2 cells was cultivated at 7×10^5 cell ml^{-1} in 75 ml DMEM, 10% FBS, 1% P/S, in a silanized 125 ml spinner vessel (from Wheaton) equipped with ball impeller. On day two, 50 ml of fresh medium was added. After three days, differentiation was induced by incubation with 10 μM retinoic acid (RA), for three weeks. During the differentiation period, a 50% medium exchange was performed every two to three days, with DMEM containing 10% FBS, 1% P/S and 20 μM RA.

Preparation of liver microtissues was performed as described in Wagner et al. (2013). In brief, 20 μl cell suspension containing 4.8×10^4 HepaRG cells and 0.2×10^4 primary human hepatic stellate cells (HHSteC) were added to each access hole of a Perfecta3D® 384-Well Hanging Drop Plate (3D Biomatrix, Ann Arbor, MI, USA). After two days of hanging drop culture, the spheroids were transferred to ultra-low attachment 24-well plates (Corning, Lowell, MA, USA) with a maximum of 20 spheroids per well.

2.3. Multi-organ chip manufacturing and culture

Fabrication of the MOC was performed as described in Wagner et al. (2013). In brief, applying replica moulding of polydimethylsiloxane (PDMS) resulted in a single 2 mm high PDMS layer containing the respective microfluidic channel system, which was permanently bonded to a glass microscope slide (Menzel, Braunschweig, Germany) using low pressure plasma oxidation (Femto; Diener, Ebhausen, Germany). The PDMS layer consisted of two compartments for cultivating cells and three pump membranes (thickness: 500 μm). A pumping frequency of 1.5 Hz and a pressure of 0.6 bar was applied.

Liver microtissues (20 spheroids per insert) and neurospheres (80 spheroids per insert), each in 350 μl HepaRG medium, were loaded into separate culture compartments of each MOC circuit for co-culture. Additional MOCs were loaded only with liver microtissues or neurospheres for comparison (Fig. 1). During the first five days, a 40% media exchange rate was applied at 12 h intervals. Later, a 40% exchange rate was applied every 24 h. Daily media samples were collected for lactate dehydrogenase (LDH), glucose and lactate

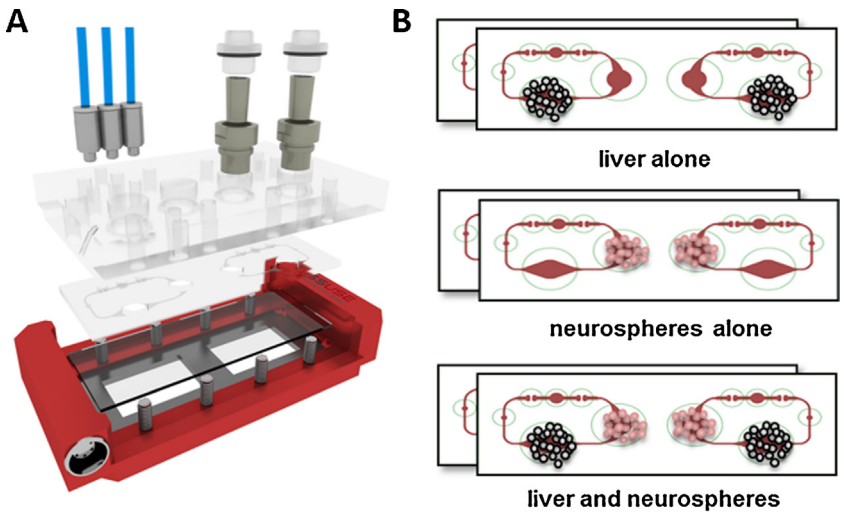

Fig. 1. The multi-organ chip. (A) Exploded view of the device comprising the PDMS-glass chip accommodating two microfluidic circuits. (B) Experimental set up of single cultivation and co-cultivation of neurospheres and liver microtissues in the MOC ($n = 4$).

analysis. Experiments were stopped at day 14 of co-culture and tissues of the MOCs were frozen in O.C.T.™ Compound at −80 °C for immunohistochemical analysis and RNA extraction.

MOC co-cultures and respective single-tissue cultures were treated with two doses of 2,5-hexanedione (≥98%) (16 mM and 32 mM) (Sigma–Aldrich, St. Louis, MO, USA) diluted in HepaRG medium from day six onwards. The concentration of 32 mM has been reported previously to lead to toxicity in NT2 cells after 24 h of administration (Woehrling et al., 2006). The HepaRG medium without any substance was used as a control.

2.4. Daily tissue culture analyses

All absorbance-related measurements were performed in 96-well microtitre-plates (Greiner Bio-One, Frickenhausen, Germany) in a microplate-reader (FLUOstar Omega, BMG Labtech, Ortenberg, Germany).

Tissue viability was measured as LDH activity in the medium, using the LDH Liqui-UV kit (Stanbio Laboratory, Boerne, USA) according to the manufacturer's instructions with minor modifications: 100 μl of reagent was preheated to 37 °C and 5 μl of medium sample was added for each measurement. The average absorbance per minute (ΔA/min) at 450 nm was determined over three minutes using medium as a reference.

Metabolic activity of the tissues in the MOC was measured as glucose consumption, using the Glucose LiquiColor® Oxidase kit (Stanbio Laboratory, Boerne, USA) with minor modifications: 100 μl of reagent was used and 1 μl of sample was added. The prepared 96-well microtitre-plate was incubated at 37 °C for 10 min. Absorbance was measured at 500 nm, using Glucose Standard, 100 mg/dl, as a reference.

Lactate concentration of the medium was measured using the LAC 142 kit, according to the manufacturer's instructions with minor modifications: 100 μl of the reagent was mixed with 1 μl of sample and incubated for 5 min at room temperature. Absorbance was measured at 520 nm, using standards (2 mM/ml, 4 mM/ml and 10 mM/ml) as a reference.

2.5. End-point tissue culture analyses

At the end of each MOC experiment, ten-micron cryostat tissue sections of neurosphere were stained for neuronal markers (βIII-tubulin and MAP2) and the human pluripotent stem cell marker TRA-1-60. Liver tissue sections were stained for cytochrome P450 3A4, the transporter multidrug resistance protein 2 (MRP-2), and for the structural proteins cytokeratin 8/18 and vimentin. Briefly, representative central cryosections of the tissues were fixed in acetone at −20 °C for 10 min, washed with PBS and blocked with 10% (v/v) goat serum in PBS for 20 min. Neurosphere sections were then incubated with mouse anti-human MAP2 (Sigma–Aldrich, St. Louis, MO, USA), mouse anti-human βIII-tubulin (eBioscience, San Diego, USA) or mouse anti-human TRA-1-60 (eBioscience, San Diego, USA) antibody overnight and washed with PBS. Subsequently, goat anti-mouse IgG Alexa Fluor® 594 (Life Technologies, Darmstadt, Germany) secondary antibodies and DAPI were added, and the sections were incubated for 45 min before fluorescence imaging. The same procedure was carried out for liver equivalents using mouse anti-human cytochrome P450 3A4, rabbit anti-human MRP-2, mouse anti-human cytokeratin 8/18, and rabbit anti-human vimentin (all antibodies purchased from Santa Cruz Biotechnology, Heidelberg, Germany). Conjugated secondary antibodies goat anti-mouse IgG Alexa Fluor® 594, goat anti-rabbit IgG Alexa Fluor® 594 and goat anti-rabbit IgG Alexa Fluor® 488 (all purchased from Life Technologies) were used for visualization. All fluorescence imaging was performed with a Keyence fluorescence microscope.

Furthermore, apoptosis and proliferation were analysed by immunohistological end-point stainings using TUNEL (TdT-mediated dUTP-digoxigenin nick end labelling)/Ki67 markers. Briefly, representative eight-micron cryostat central sections of the tissue were stained for apoptosis using the TUNEL technique (ApopTag1 Peroxidase In Situ Apoptosis Detection Kit, Merck Millipore, Darmstadt, Germany) according to the manufacturer's instructions. The apoptosis staining was combined with a nuclear stain, Hoechst 33342 (Life Technologies, Darmstadt, Germany), and an antibody Ki67 (Abcam, Cambridge, UK).

Tissues embedded in O.C.T.™ Compound were cut to 50 μm slices, 400 μl RA1 buffer containing 1:1000 β-mercaptoethanol (Sigma–Aldrich, St. Louis, MO, USA) was added onto the slices and RNA was collected using the NucleoSpin RNA XS kit (Macherey-Nagel, Düren, Germany) according to the manufacturer's instructions for real-time quantitative PCR (qRT-PCR) end-point analyses. cDNA was synthesized by reverse transcription of 200–400 ng total RNA using TaqMan Reverse Transcription Reagents cDNA kit (TaqMan®, Roche Diagnostics, Mannheim, Germany). qRT-PCR experiments were conducted by using the Stratagene system (Agilent Technologies, Böblingen, Germany) and

Table 1
Primer sequences used for qPCR.

Primer	Forward	Reverse
βIII-tubulin	CAGCAAGGTGCGTGAGGAG	TGCGGAAGCAGATGTCGTAG
Oct 4	GACAACAATGAGAACCTTCAGGAGA	CTGGCGCCGGTTACAGAACCA
Pol2	CAGTGTTGGGAGTGGAATGACC	GTGAAGGGATGTAGGGGCTTG
Nestin	GGCAGCGTTGGAACAGAGGTTGGA	CTCTAAACTGGAGTGGTCAGGGCT
Albumin	TGCAAGGCTGACGATAAGGAG	TTTAGACAGGGTGTTGGCTTTACAC
BSEP	GCAGACACTGGCGTTTGTTG	ATGTTTGAGCGGAGGAACTGG
CPS-1	CCCAGCCTCTCTTCCATCAG	GCGAGATTTCTGCACAGCTTC
Cyp 1A2	ATCCCCCACAGCACAACAAG	CCATGCCAAACAGCATCATC
Cyp 2B6	ACCAGACGCCTTCAATCCTG	GGGTATTTTGCCCACACCAC
Cyp 3A4	GGAAGTGGACCCAGAAACTGC	TTACGGTGCCATCCCTTGAC
TBP	CCTTGTGCTCACCCACCAAC	TCGTCTTCCTGAATCCCTTTAGAATAG

the SensiFast SYBR No-ROX One-Step kit (Bioline, Luckenwalde, Germany), according to the manufacturer's instructions. The list of primers used and their sequences are presented in Table 1. Cycle threshold and melting curves were determined using LightCycler software and results were processed using the 2-ΔΔCt method for relative gene expression analysis (Brito et al., 2012; Livak and Schmittgen, 2001). Changes in gene expression were normalized using the housekeeping gene TBP (liver spheroids) and Pol2 (neurospheres). qRT-PCR of neurospheres was performed as described in Brito et al. (2012). Briefly, total RNA was extracted with a High Pure RNA Isolation kit (Roche) and quantified using a NanoDrop 2000c (ThermoScientific). Reverse transcription was performed with a Transcriptor High Fidelity cDNA Synthesis kit (Roche), using Anchored-oligo(dT)18 Primer. qRT-PCR analysis was performed in a LightCycler 480 Multiwell Plate 96 (Roche), according to LightCycler 480 SYBR Green I Master Kit (Roche). cDNA was diluted 1:2 and primers were used in a concentration of 5 μM, in 20 μl reactions; each sample was performed in triplicate. The list of primers used and their sequences is presented in Table 2. Cycle threshold and melting curves were determined using LightCycler 480 software, version 1.5 (Roche) and results were processed using the 2-ΔΔCt method for relative gene expression analysis (Brito et al., 2012; Livak and Schmittgen, 2001). Changes in gene expression were normalized using the housekeeping gene RPL22 (coding for ribosomal protein L22) as an internal control.

3. Results

3.1. Characterization of neurospheres

Neurospheres were reproducibly differentiated from NT2 undifferentiated cells as 3D aggregates in stirred suspension culture system, forming compact and spherical structures typical of neurosphere cultures (Serra et al., 2009), with a medium diameter of 179.0 ± 76.5 μm. The structural integrity of the spheroids was maintained during culture time, with high cell viability and no evidences of necrotic cores, as indicated by generalized FDA staining and few PI-positive cells distributed through the spheroids (Fig. 2b).

Cultures were monitored during differentiation to characterize NT2-derived cells. Expression of nestin, a marker of undifferentiated NT2 cells and early neuroepithelial progenitors, was four-fold upregulated until day 10 (Fig. 2f). Concomitantly, an eight-fold increase in the expression of the neuronal marker βIII-tubulin was observed between days 3 and 10 (Fig. 2g), probably corresponding to the proliferation of nestin and βIII-tubulin positive neuronal progenitors. Nestin expression decreased from day 10 onwards (Fig. 2f) while βIII-tubulin maintained high expression levels (Fig. 2g), indicating an efficient differentiation towards the neuronal lineage. In accordance, immunostaining at day 24 showed an extensive network of βIII-tubulin-positive cells (Fig. 2c). Moreover, detection of MAP2-positive cells throughout the neurospheres indicated that these neurons were acquiring mature neuronal phenotypes (Fig. 2d). Gene expression of synaptophysin, a presynaptic vesicle glycoprotein, displayed a six-fold increase during the 24 days of differentiation (Fig. 2h); moreover, the protein was detected in neurites, with a punctate pattern, consistent with pre-synaptic vesicle enrichment (Fig. 2e). Detection of MAP2-positive neurons and the increase in synaptophysin gene expression during differentiation, with accumulation of synaptophysin-positive vesicles, suggest that neuronal differentiation occurred within the neurospheres.

Table 2
Primer sequences used for qRT-PCR analysis of neurospheres.

Primer	Forward	Reverse
RPL22	CACGAAGGAGGAGTGACTGG	TGTGGCACACCACTGACATT
Nestin	TAAGGTGAAAAGGGGTGTGG	GCAAGAGATTCCCTTTGCAG
βIII-tubulin	GGGCCTTTGGACATCTCTTC	CCTCCGTGTAGTGACCCTTG
Synaptophysin	TTTGTGAAGGTGCTGCAATG	GCTGAGGTCACTCTCGGTCT

3.2. Characterization of liver spheroids produced from HepaRG and HHSteC

HepaRG cells were pre-differentiated in monolayer cultures, as described by Gripon et al. (2002). These cells, known for their capacity to form bile-canalicular structures in culture, excreted carboxyfluorescein diacetate into defined spaces between cells suggestive of functional canaliculi (Fig. 3b). After differentiation, cells were combined with HHSteC for the production of liver spheroids.

Liver spheroids with a medium diameter of 300–400 μm and a height of 200–300 μm were reproducibly formed during the two-day hanging drop co-culture. Immunofluorescence staining of newly formed spheroids for cytokeratin 8/18 and vimentin revealed that HHSteCs were homogenously distributed throughout the spheroids (Fig. 3c). MRP-2 is selectively transported to the apical membrane of bile canaliculi in hepatocytes. Here, the existence of MRP-2 surrounding the cells indicated that cells in the generated microtissues had started to reform canalicular-like structures as previously observed for monolayer cultures. However, staining was weak, indicating a non-complete reformation of bile canaliculi (Fig. 3d). Moreover, qPCR analysis of functional markers albumin, canalicular transport protein bile salt export pump (BSEP), urea cycle enzyme carbamoyl phosphate synthetase 1 (CPS-1), and phase I metabolizing cytochrome P450 (Cyp) enzymes revealed an up to twenty-fold increase after differentiation towards the hepatic lineage, which was maintained in spheroids (Fig. 3e–k). Only the expression of Cyp 3A4 showed a significant decrease in spheroids compared to differentiated monolayer cultures. This is probably due to the fact that the spheroids were no longer treated with DMSO, a known Cyp 3A4 inducer. However, a three-day treatment with rifampicin showed that Cyp 3A4 and 2B6 enzyme expression in spheroids was inducible (Fig. 3i,k).

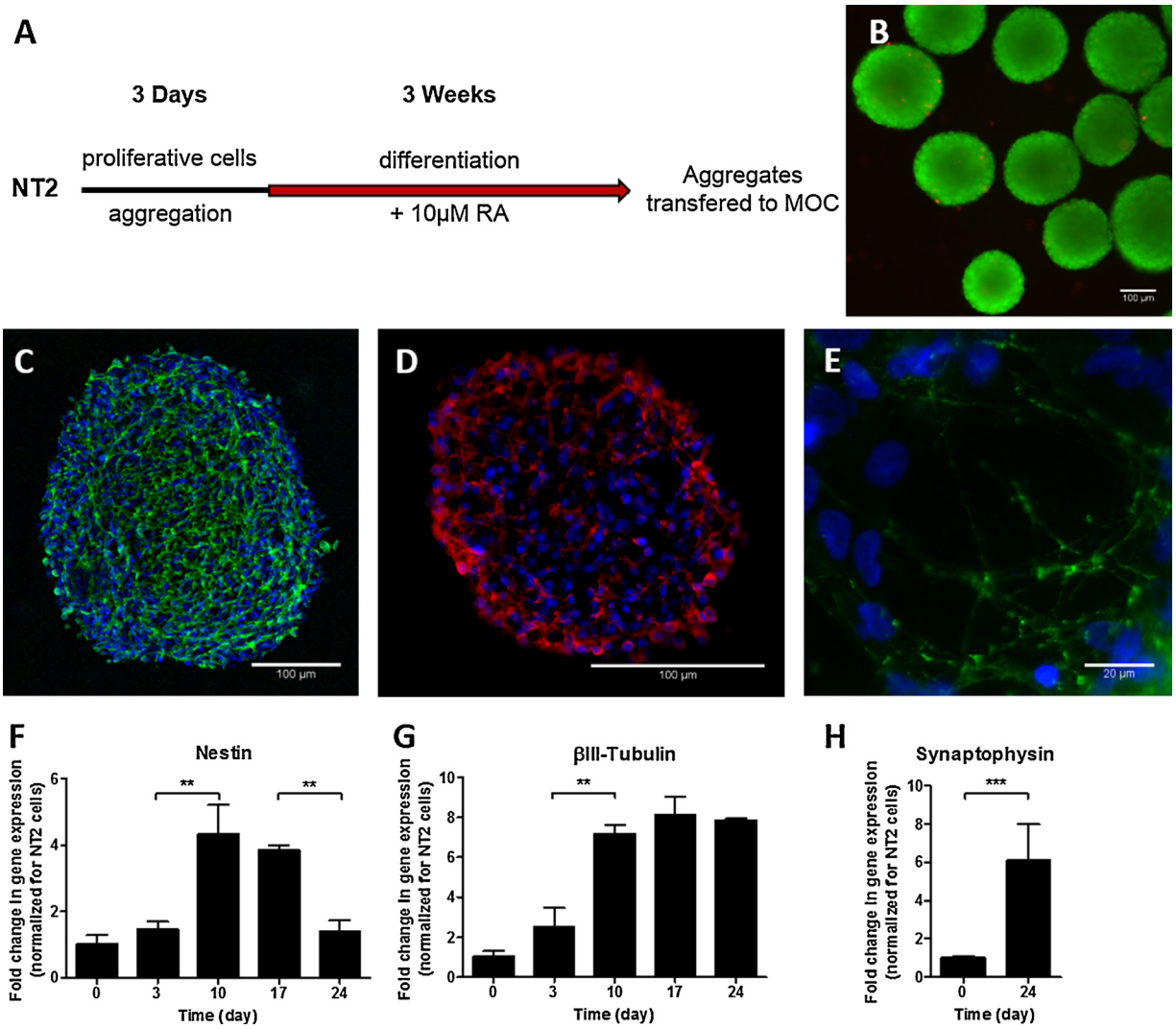

Fig. 2. Preparation, differentiation and characterization of neurosphere cultures. (A) Schematic workflow of stirred suspension culture. Cells were inoculated in a stirred suspension culture system and aggregated for three days. Neural differentiation was induced by retinoic acid (RA) for three weeks. (B) Image representative of the culture status at the end of RA-induced differentiation: fluorescent live/dead assay using fluorescein diacetate for identification of live cells (green) and propidium iodide for identification of dead cells (red). (C–E) Immunostaining of neurospheres at the end of RA-induced differentiation: (C) βIII-tubulin (green), (D) MAP2 (red) and (E) synaptophysin (green). Nuclei were stained with DAPI (blue). (F-H) qRT-PCR analysis of (F) nestin, (G) βIII-tubulin and (H) synaptophysin gene expression. The fold changes of mRNA concentration of the neurospheres during the culture are represented, relative to NT2 undifferentiated cells; data are mean ± SD of three independent cultures. Asterisks indicate significant difference ($P < 0.01$) by Mann-Whitney test. Scale bars B, C, D: 100 µm, E: 20 µm. (For interpretation of the color information in this figure legend, the reader is referred to the web version of the article.)

3.3. Neurosphere-liver co-cultivation in the MOC over 14 days

A successful co-cultivation of neurospheres and liver microtissues in the MOC system was performed over 14 days. A constant LDH activity in the medium supernatant over the whole cultivation period of 14 days indicated a stable tissue turnover and cell viability (Fig. 6). Glucose consumption and lactate production were measured as indicators of metabolic activity in the MOC. Both decreased during the first days of co-culture, reaching a steady state with low fluctuations from day six onwards. The neurospheres changed their morphology during the cultivation in the perfused MOC, attaching to the glass bottom of the chip. The neurospheres grew out, fused together and formed an almost multilayer-like structure over two weeks. The shear stress of 1.5 Hz enhanced the levelling and fusion of the spheres. Liver microtissues only slightly changed their morphology during the two weeks of cultivation, maintaining their 3D spheroid structure, but also attached to the glass bottom and fused to some extend to other spheroids. Immunohistological end-point staining of neurosphere samples were highly positive for the neuronal marker MAP2 and βIII-tubulin (Fig. 4d,e). The intensity of the staining was comparable to the control neurospheres at day zero, which were not cultivated in the MOC. The embryonic stem cell marker TRA-1-60 was negative in all samples (Fig. 4f). Liver spheroids stained for cytokeratin 8/18 and vimentin showing that HHSteC were still homogenously distributed throughout the spheroids (Fig. 4a). Furthermore, staining for cytochrome P450 3A4 and MRP-2 was intense, suggesting a well differentiated phenotype (Fig. 4b,c). qRT-PCR analysis supported these findings and showed that expression of functional markers albumin, cytochrome P450 2B6 and 3A4 increased five- to fifteen-fold when cultured in the MOC for 14 days (Fig. 5a–c). The co-culture with neurospheres did not show any significant effects on the differentiated status of liver equivalents (Fig. 5a–c). Furthermore, the differentiated state of the neurospheres was maintained in MOC cultures compared to day 0 spheroids, as shown by nestin, βIII-tubulin and Oct 4 expression (Fig. 5d–f).

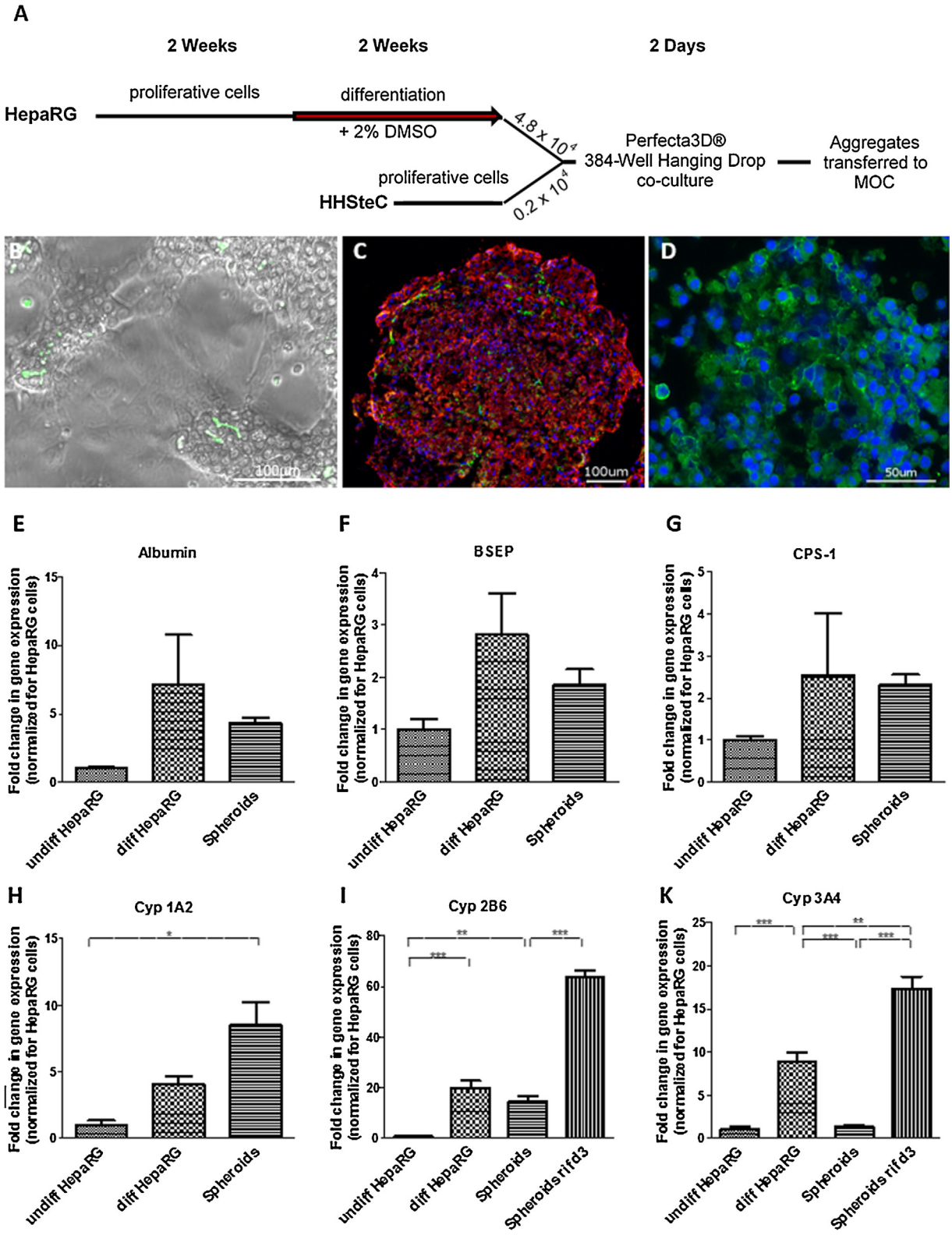

Fig. 3. Preparation, differentiation and characterization of liver spheroids. (A) Schematic workflow of liver spheroid production. HepaRG cells were differentiated, mixed with HHSteC and aggregated for two days. Hepatic differentiation was induced by dimethyl sulfoxid (DMSO) for two weeks. (B) Microscopic image of HepaRG monolayer treated with carboxyfluorescein diacetate. Green fluorescence shows bile canaliculi. C, D Immunostaining of representative aggregates after aggregation procedure: (C) vimentin (red) and cytokeratin 8/18 (green) and (D) MRP-2 (green). Nuclei were stained with DAPI (blue). qRT-PCR analysis of E. albumin, F. BSEP, G. CPS-1, H. cytochrome P450 1A2, I. cytochrome P450 2B6 and K. cytochrome P450 3A4 gene expression. The fold changes of mRNA concentration of differentiated HepaRG cells (diff HepaRG), newly formed spheroids (Spheroid) and spheroids treated for three days with rifampicin (Spheroids rif d3), relative to undifferentiated HepaRG cells (undiff HepaRG), are represented; data are mean ± SD of four independent cultures. Asterisks indicate significant difference ($^{*}p \leq 0.05$, $^{**}p \leq 0.01$, $^{***}p \leq 0.001$) by one-way ANOVA analysis with Tukey's post multiple comparison test. Scale bars B, C: 100 µm, D: 50 µm. (For interpretation of the color information in this figure legend, the reader is referred to the web version of the article.)

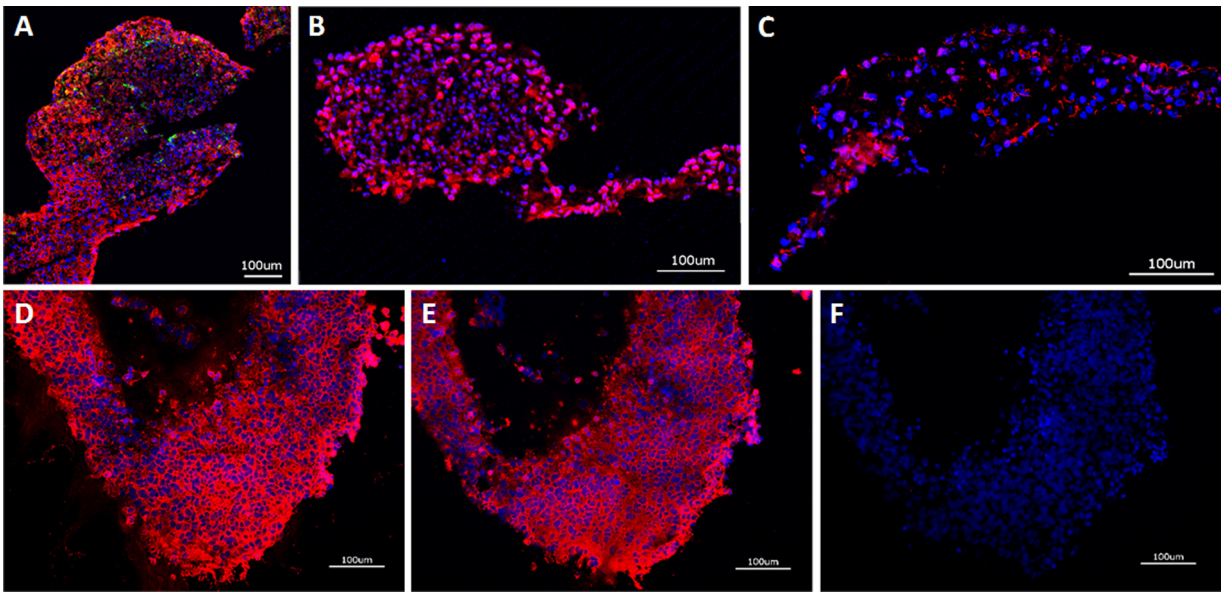

Fig. 4. Immunostaining of co-cultures after 14 days of MOC cultivation. Liver spheroids were stained for (A) cytokeratin 8/18 (red) and vimentin (green), (B) cytochrome P450 3A4 (red) and (C) MRP-2 (red). The neurospheres were stained for (D) βIII-tubulin (red), (E) MAP2 (red) and (F) TRA-1-60 (red). Nuclei are stained with DAPI (blue). Scale bars: 100 μm. (For interpretation of the color information in this figure legend, the reader is referred to the web version of the article.)

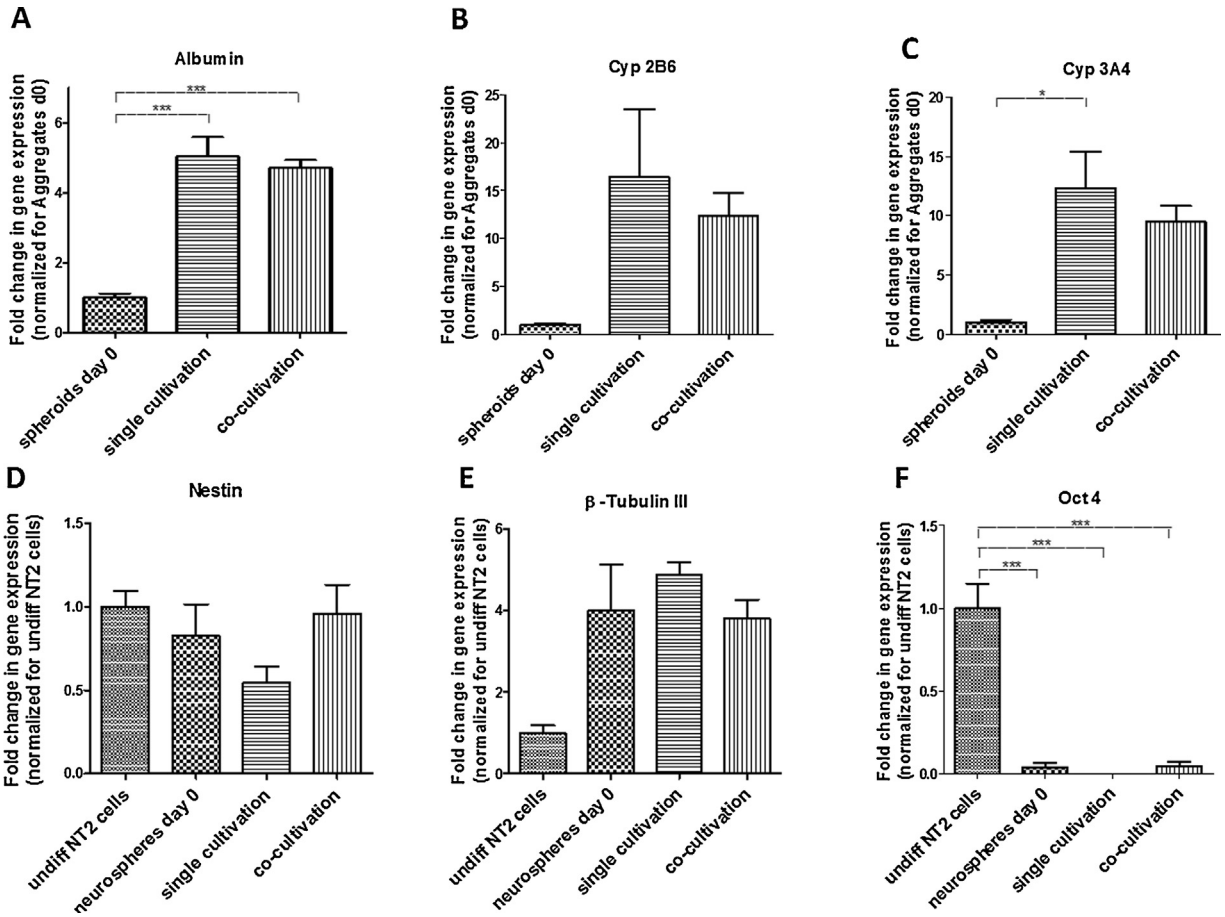

Fig. 5. qPCR results of liver spheroids and neurospheres after single cultivation and co-cultivation in the MOC for 14 days. (A) albumin, (B) cytochrome P450 2B6 and (C) cytochrome P450 3A4 gene expression in liver spheroids. (D) nestin, (E) βIII-tubulin and (F) Oct 4 gene expression in neurospheres. Data represent the fold changes of mRNA concentration of single cultivated and co-cultivated liver spheroids and neurospheres relative to day 0 spheroids (spheroid day 0) or undifferentiated NT2 cells (undiff NT2 cells); data are mean ± SD of three independent co-cultures. Asterisk $^{*}p \leq 0.05$, $^{***}p \leq 0.001$ by one-way ANOVA analysis with Tukey's post multiple comparison test.

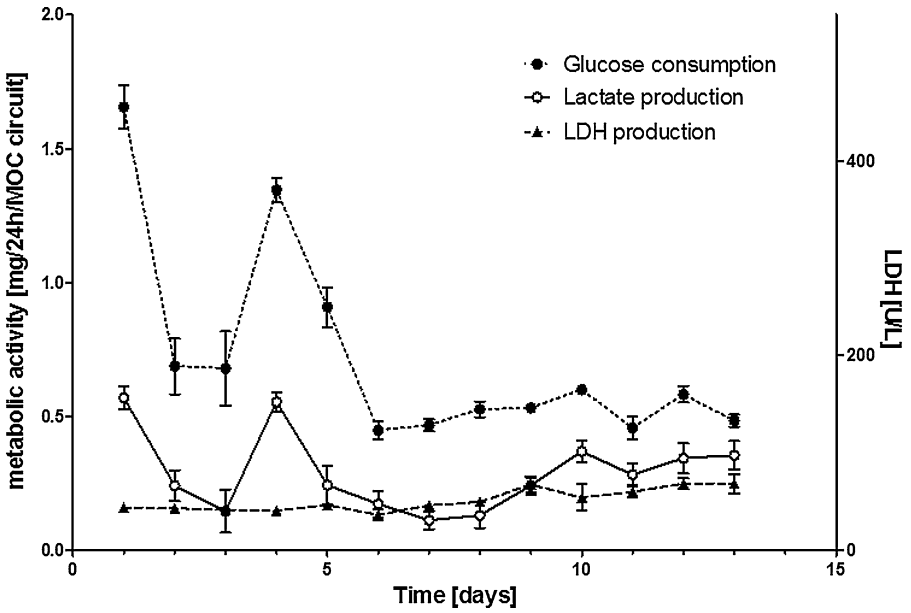

Fig. 6. 14-day tissue performance of co-cultures in the MOC. Metabolic activity of tissues assessed by glucose consumption and lactate production. LDH activity in the media supernatant was constantly low over the whole cultivation period; data are mean ± SD of three independent co-cultures.

3.4. Toxicity study of neurosphere-liver equivalent co-cultivation in the MOC

MOC co-cultures of liver equivalents and neurospheres were treated with 2,5-hexanedione to observe tissue interactions during a toxic insult. Control MOCs, which were not treated with the substance, showed a constant LDH activity of about 50 U/L in the medium over the whole cultivation time (Fig. 7a). These values were identical to those of treated cultures until day six, when daily addition of substance started, again, indicating a stable and viable multi-tissue co-culture. The dose-dependent effect of 2,5-hexanedione on the co-culture of the neurospheres and liver equivalents was demonstrated by a significant increase in LDH activity starting from day seven or nine in cultures treated with 32 mM or 16 mM, respectively. On day 10, the LDH concentration of co-cultures treated with 32 mM 2,5-hexanedione decreased again, indicating that most of the cells had already lysed. The increase of the LDH activity in cultures treated with 16 mM was delayed by two days, however, after reaching a maximum of 200 U/l, it also decreased again.

Treating single-tissue MOC cultures of neurospheres and liver equivalents with 2,5-hexanedione and comparing them the co-cultures revealed that co-cultivated tissues were more sensitive to 2,5-hexanedione than the sum of the single cultivated neurospheres and liver equivalents (Fig. 7b). This effect was especially pronounced in the co-cultures treated with 16 mM 2,5-hexanedione at day 9 and 10.

Furthermore, single-tissue MOC cultures of liver equivalents showed a higher sensitivity to 2,5-hexanedione than the neurospheres (Fig. 7c,d). The dose-dependent effect of 2,5-hexanedione was also observed on those MOC cultures.

Staining for TUNEL/Ki67 revealed that proliferating cells were evenly distributed in neurospheres and liver spheroids on day zero as well as after 14 days of MOC co-cultivation. Whereas, treatment with 2,5-hexanedione led to a strong increase in apoptotic cells in the tissue models (Fig. 8).

4. Discussion

Microfluidic platforms have proven to be a stable and powerful tool for cultivating tissues of various origins under stable extracellular conditions (Griffith et al., 1997; Huh et al., 2012; Marx et al., 2012; Materne et al., 2013). The multi-organ chip platform used in this study enabled a co-culture of well-defined neurospheres and liver equivalents in a connecting media circuit under dynamic flow conditions over 14 days. Cells were viable, showed tissue specific expression of markers and were able to respond to a toxic insult by 2,5-hexanedione. To the best of our knowledge, this is the first time a liver-neurosphere co-culture in a microfluidic device has been performed over 14 days.

In recent years, tissue engineering paradigms have revolutionized a shift from two-dimensional *in vitro* test systems towards three-dimensional tissue equivalents for substance testing. These complex structures, often composed of multiple cell-types and integrating technologies, such as biomaterial sciences, are a closer model of human physiology and, therefore, lead to a higher predictability of clinical outcomes (Wu et al., 2010). Even though these systems are often more time-consuming and cost-intensive during production, they enable high content analysis of mode of action of substances in near physiological cellular environments (Esch et al., 2011; Hwan et al., 2009). The integration of various cell types into organoid-like structures allows the cells to interact and differentiate towards mature phenotypes (Abu-Absi et al., 2004; Krause et al., 2009). We previously developed techniques to aggregate differentiated HepaRG cells with HHSteC in hanging drop plates. These spheroids were shown to express liver-typical markers at levels comparable to or even higher than differentiated monolayer cells, even though the spheroids were no longer stimulated with DMSO. The inducibility of cytochrome P450 enzymes in spheroids suggests a metabolically competent phenotype. The aggregation and neuronal differentiation of NT2 cells in stirred suspension culture systems was developed previously by Serra et al. (2009). These neurospheres were shown to acquire mature neuronal phenotype features, such as MAP2 and vesicular synaptophysin staining during a three-week differentiation procedure, enabling screening the effects of potentially neurotoxic substances.

These two complex tissues were combined in a common media circulation to increase model complexity, taking a further step towards the final goal of predicting adverse outcome pathways. Under standard *in vitro* culture conditions, three-dimensional tissue models often dedifferentiate over time as a result of limited oxygen and nutrient supply to the cells (Goral et al., 2010; Prot

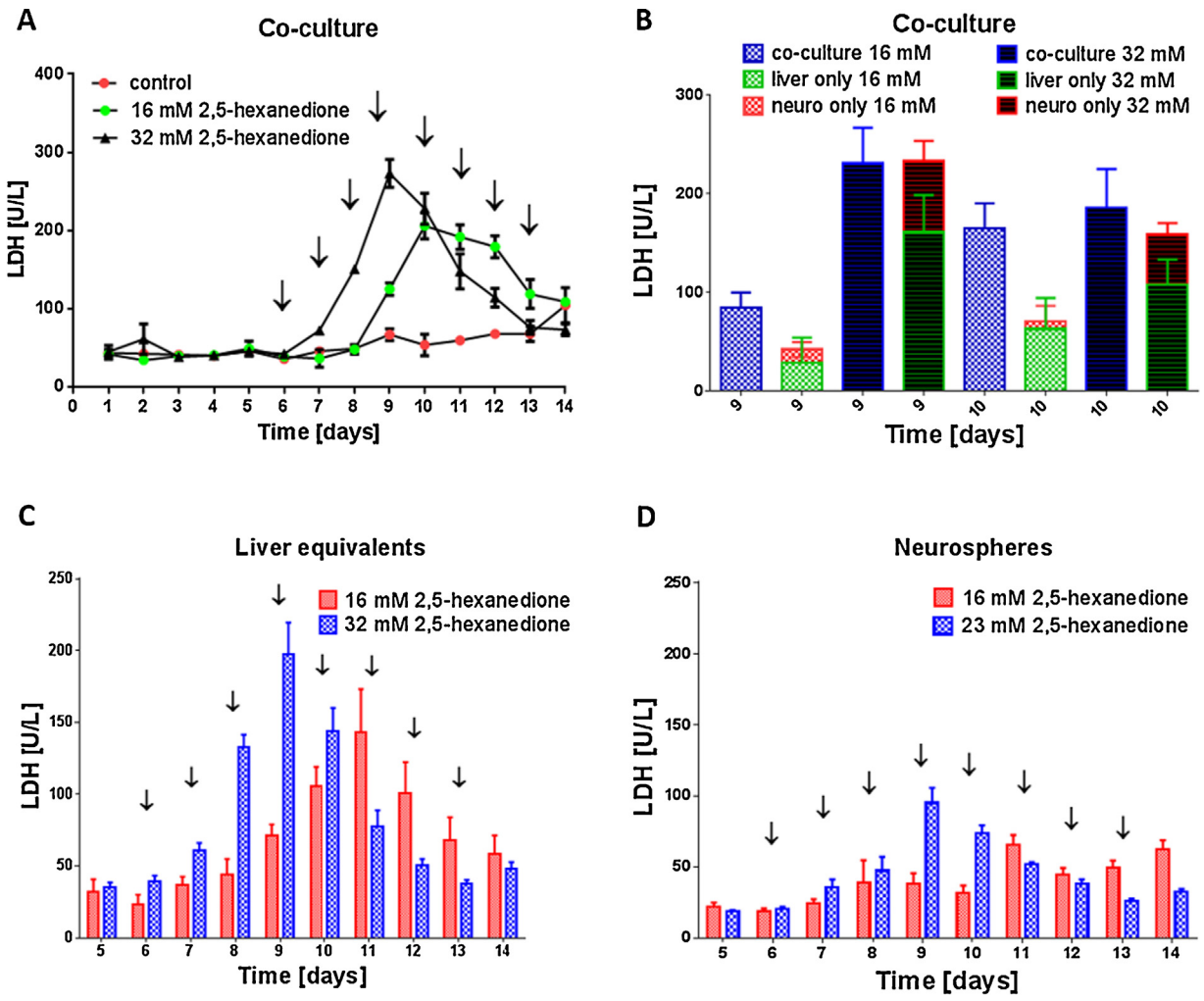

Fig. 7. LDH activity in media supernatants of untreated and treated cultures. Co-cultures were exposed to 0, 16 mM or 32 mM 2,5-hexanedione for eight days starting on day six of culture. (A) Time course of LDH activity in media supernatants of co-cultures. (B) LDH activity in media supernatants of co-cultures (co-culture) and sum of LDH activities of liver and neuronal single-tissue MOC cultures (liver only, neuro only) on day 9 and 10 of culture. Time course of LDH activity in media supernatants of (C) Liver single-tissue MOC culture and (D) neurosphere single-tissue MOC culture. (A), (C), (D): Arrows depict substance application; data are mean ± SD of four independent cultures.

et al., 2011). This leads to a low predictability of the effects of substances on the respective organs during pre-clinical toxicity tests. Whereas, the continuous mixing of substances through perfusion in microfluidic systems leads to a better control of parameters such as the removal of cellular excretions and physical stimuli reaching the cells. The combination of two different organ systems in one media circuit enabled the tissues to communicate through secreted factors. Furthermore, the effects of substances being metabolized by the liver and reaching the neuronal system thereafter can be studied.

One of the most important requirements for future systemic substance testing is the ability of metabolites to reach secondary organ systems (Viravaidya and Shuler, 2004). The high fluid-to-tissue ratios of most microfluidic systems may pose a challenge in effective cellular communication, as most secreted factors are diluted within the high medium volume (Wikswo et al., 2013). The MOC platform used in this study comprises an on-chip micropump, eliminating the need for external media reservoirs. This enables the chip to run at very low medium volumes, allowing for cellular interaction. However, metabolic activities, measured as glucose consumption and lactate production, of the neurosphere-liver co-culture demonstrated that a stable homeostasis was achieved after six days of cultivation. Furthermore, proliferating cells were still found in both tissues after 14 days of co-cultivation in the MOC. These results suggest that the small medium volume was able to sustain both tissues, supplying sufficient nutrient and oxygen to the cells. It is interesting that the LDH activity in the medium stayed constant over the whole cultivation time, indicating a stable tissue turnover. Furthermore, the differentiated state of the tissues was not altered by the co-culture, as shown by qRT-PCR.

The principal finding of the exposure of the co-culture to 2,5-hexanedione was that not only toxicity profiles of two different doses could be discriminated, but also that the co-cultures were more sensitive to the substance compared to single-tissue cultures. We hypothesize that necrotic signals from one tissue culture might have led to an intensification of the response in the second culture. This hypothesis is backed by the fact that the increased sensitivity of the co-cultures was primarily found in cultures exposed to the lower concentration of the substance. Co-cultures exposed to higher concentrations showed no such intensified effects.

In conclusion, we have demonstrated that highly differentiated neurospheres and liver spheroids could be co-cultivated in a combined media circuit over 14 days retaining the cells differentiated phenotype. Furthermore, as discussed above, we have shown that the sensitivity of co-cultures towards 2,5-hexanedione, probably due to tissue-tissue communication, was increased compared to single-tissue cultures. However, further studies elucidating the mechanism behind this phenomenon are required.

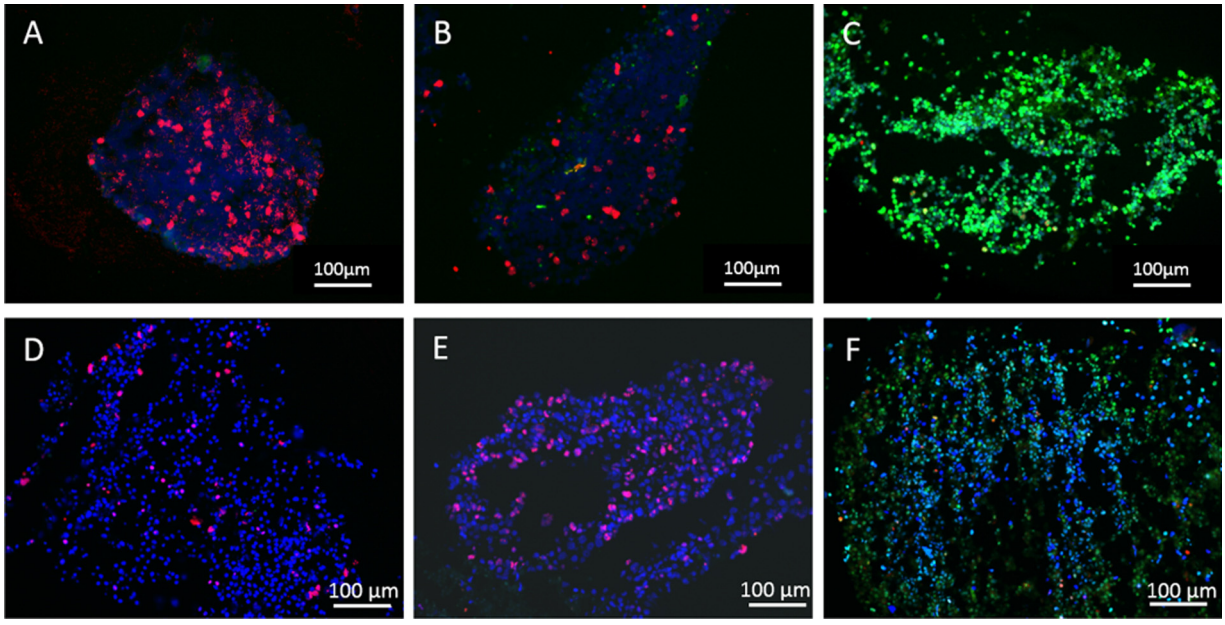

Fig. 8. TUNEL/Ki67 staining of tissue models. TUNEL (green) and Ki67 (red) immunohistochemical staining of A-C. neurospheres and D-F. liver spheroids. A, D. Control tissue from day zero, which were not cultivated in the MOC. B, E. Co-cultured microtissues in the MOC for 14 days. C, F. Tissues co-cultured in the MOC for 14 days and exposed to 2,5-hexanedione for 8 days. Nuclei are stained with DAPI (blue). Scale bars: 100 µm. (For interpretation of the color information in this figure legend, the reader is referred to the web version of the article.)

Disclosure

Uwe Marx is CEO of TissUse GmbH that produces and markets the Multi-Organ-Chip platform used in the article.

Acknowledgments

The work was supported by the German Federal Ministry for Education and Research, GO-Bio Grant No. 0315569 and by Fundação para a Ciência e Tecnologia (FCT), Portugal, under the scope of the project PTDC/EBB-BIO/112786/2009 and by the Ph.D. fellowship to A.P.T., SFRH/BD/52473.

References

Abu-Absi, S.F., Hansen, L.K., Hu, W.-S., 2004. Three-dimensional co-culture of hepatocytes and stellate cells. Cytotechnology 45 (125-40.), http://dx.doi.org/10.1007/s10616-004-7996-6.

Bailey, J., Thew, M., Balls, M., 2013. An analysis of the use of dogs in predicting human toxicology and drug safety. ATLA 1, 335–350.

Brito, C., Escrevente, C., Reis, C.A., Lee, V.M., Trojanowski, J.Q., 2007. Increased levels of fucosyltransferase IX and carbohydrate lewis × adhesion determinant in human NT2N neurons. J. Neurosci. Res. 1270, 1260–1270, http://dx.doi.org/10.1002/jnr.

Brito, C., Simão, D., Costa, I., Malpique, R., Pereira, C.I., Fernandes, P., Serra, M., Schwarz, S.C., Schwarz, J., Kremer, E.J., Alves, P.M., 2012. Generation and genetic modification of 3D cultures of human dopaminergic neurons derived from neural progenitor cells. Methods 56, 452–460.

DeCaprio, A.P., Briggs, R.G., Jackowski, S.J., Kim, J.C.S., 1988. Comparative neurotoxicity and pyrrole-forming potential of 2,5-hexanedione and perdeuterio-2,5-hexanedione in the rat. Toxicol. Appl. Pharmacol. 92, 75–85.

Dragunow, M., 2008. The adult human brain in preclinical drug development. Nat. Rev. Drug Discov. 7, 659–666, http://dx.doi.org/10.1038/nrd2617.

Esch, M.B., King, T.L., Shuler, M.L., 2011. The role of body-on-a-chip devices in drug and toxicity studies. Annu. Rev. Biomed. Eng. 13, 55–72, http://dx.doi.org/10.1146/annurev-bioeng-071910-124629.

Gibbons, H.M., Dragunow, M., 2010. Adult human brain cell culture for neuroscience research. Int. J. Biochem. Cell Biol. 42, 844–856, http://dx.doi.org/10.1016/j.biocel.2009.12.

Goral, V.N., Hsieh, Y.-C., Petzold, O.N., Clark, J.S., Yuen, P.K., Faris, R., a, 2010. Perfusion-based microfluidic device for three-dimensional dynamic primary human hepatocyte cell culture in the absence of biological or synthetic matrices or coagulants. Lab Chip 10, 3380–3386, http://dx.doi.org/10.1039/c0lc00135j.

Griffith, L.G., Wu, B., Cima, M.J., Powers, M.J., Chaignaud, B., Vacanti, J.P., 1997. In vitro organogenesis of liver tissue. Ann. N. Y. Acad. Sci. 831, 382–397.

Gripon, P., Rumin, S., Urban, S., Le Seyec, J., Glaise, D., Cannie, I., Guyomard, C., Lucas, J., Trepo, C., Guguen-Guillouzo, C., 2002. Infection of a human hepatoma cell line by hepatitis B virus. Proc. Natl. Acad. Sci. U.S.A. 99, 15655–15660, http://dx.doi.org/10.1073/pnas.232137699.

Heijink, E., Scholten, S.W., Bolhuis, P.A., De Wolff, F.A., 2000. Effects of 2, 5-hexanedione on calpain-mediated degradation of human neurofilaments in vitro. Chem. Biol. Interact. 129, 231–247.

Huh, D., Torisawa, Y., Hamilton, G.a., Kim, H.J., Ingber, D.E., 2012. Microengineered physiological biomimicry: organs-on-chips. Lab Chip 12, 2156–2164, http://dx.doi.org/10.1039/c2lc40089h.

Hwan, J., Shuler, M.L., Sung, J.H., 2009. A micro cell culture analog (microCCA) with 3-D hydrogel culture of multiple cell lines to assess metabolism-dependent cytotoxicity of anti-cancer drugs. Lab Chip 9, 1385–1394, http://dx.doi.org/10.1039/b901377f.

Krause, P., Saghatolislam, F., Koenig, S., Unthan-Fechner, K., Probst, I., 2009. Maintaining hepatocyte differentiation in vitro through co-culture with hepatic stellate cells. In Vitro Cell. Dev. Biol. Anim. 45, 205–212, http://dx.doi.org/10.1007/s11626-008-9166-1.

Ladefoged, O., Roswall, K., Larsen, J.-J., 1994. Acetone potentiation and influence on the reversibility of 2,5-hexanedione-induced neurotoxicity studied with behavioural and morphometric methods in rats. Pharmacol. Toxicol. 74, 294–299.

Livak, K.J., Schmittgen, T.D., 2001. Analysis of relative gene expression data using real-time quantitative PCR and the 2(-Delta Delta C(T)) Method. Methods 25, 402–408, http://dx.doi.org/10.1006/meth.2001.1262.

Marx, U., Walles, H., Hoffmann, S., Lindner, G., Horland, R., Sonntag, F., Klotzbach, U., Sakharov, D., Tonevitsky, A., Lauster, R., 2012. Human-on-a-chip developments: a translational cutting-edge alternative to systemic safety assessment and efficiency evaluation of substances in laboratory animals and man. ATLA 40, 235–257.

Materne, E.-M., Tonevitsky, A.G., Marx, U., 2013. Chip-based liver equivalents for toxicity testing–organotypicalness versus cost-efficient high throughput. Lab Chip 13, 3481–3495, http://dx.doi.org/10.1039/c3lc50240f.

Paul, S.M., Mytelka, D.S., Dunwiddie, C.T., Persinger, C.C., Munos, B.H., Lindborg, S.R., Schacht, A.L., 2010. How to improve R&D productivity: the pharmaceutical industry's grand challenge. Nat. Rev. Drug Discov. 9, 203–214, http://dx.doi.org/10.1038/nrd3078.

Prot, J.-M., Aninat, C., Griscom, L., Razan, F., Brochot, C., Guillouzo, C.G., Legallais, C., Corlu, A., Leclerc, E., 2011. Improvement of HepG2/C3A cell functions in a microfluidic biochip. Biotechnol. Bioeng. 108, 1704–1715, http://dx.doi.org/10.1002/bit.23104.

Schimek, K., Busek, M., Brincker, S., Groth, B., Hoffmann, S., Lauster, R., Lindner, G., Lorenz, A., Menzel, U., Sonntag, F., Walles, H., Marx, U., Horland, R., 2013. Integrating biological vasculature into a multi-organ-chip microsystem. Lab Chip 13, 3588–3598, http://dx.doi.org/10.1039/c3lc50217a.

Serra, M., Brito, C., Costa, E.M., Sousa, M.F.Q., Alves, P.M., 2009. Integrating human stem cell expansion and neuronal differentiation in bioreactors. BMC Biotechnol. 9, 82, http://dx.doi.org/10.1186/1472-6750-9-82.

Viravaidya, K., Shuler, M.L., 2004. Incorporation of 3T3-L1 cells to mimic bioaccumulation in a microscale cell culture analog device for toxicity studies. Biotechnol. Prog. 20, 590–597, http://dx.doi.org/10.1021/bp034238d.

Wagner, I., Materne, E.-M., Marx, U., Brincker, S., Süssbier, U., Frädrich, C., Busek, M., Sonntag, F., Sakharov, D.a, Trushkin, E.V., Tonevitsky, A.G., Lauster, R., 2013.

A dynamic multi-organ-chip for long-term cultivation and substance testing proven by 3D human liver and skin tissue co-culture. Lab Chip 13, 3538–3547, http://dx.doi.org/10.1039/c3lc50234a.

Wikswo, J.P., Curtis, E.L., Eagleton, Z.E., Evans, B.C., Kole, A., Hofmeister, L.H., Matloff, W.J., 2013. Scaling and systems biology for integrating multiple organs-on-a-chip. Lab Chip 13, 3496–3511, http://dx.doi.org/10.1039/c3lc50243k.

Woehrling, E.K., Zilz, T.R., Coleman, M.D., 2006. The toxicity of hexanedione isomers in neural and astrocytic cell lines. Environ. Toxicol. Pharmacol. 22, 249–254, http://dx.doi.org/10.1016/j.etap.2005.12.010.

Wu, M.-H., Huang, S., Lee, G.-B., 2010. Microfluidic cell culture systems for drug research. Lab Chip 10, 939–956, http://dx.doi.org/10.1039/b921695b.

Yin, H., Guo, Y., Zeng, T., Zhao, X., Xie, K., 2013. Correlation between levels of 2, 5-hexanedione and pyrrole adducts in tissues of rats exposure to n-hexane for 5-days. PLoS One 8, e76011, http://dx.doi.org/10.1371/journal.pone.0076011.

Zhang, C., Zhao, Z., Abdul, A., Noort, V., Yu, H., Abdul Rahim, N.A., van Noort, D., 2009. Towards a human-on-chip: culturing multiple cell types on a chip with compartmentalized microenvironments. Lab Chip 9, 3185–3192, http://dx.doi.org/10.1039/b915147h.